Review

Volumetric and Turbine Expander Technologies in Organic Rankine Cycle Systems: A Systematic Review

Jui-Ching Hsieh *, Hsien-Ta Tsai, Yeh-Tung Chen, Cai-Ling Chen, and Cheng-Fu Lin

Department of Mechanical Engineering, National Chin-Yi University of Technology, Taiping District, Taichung City 41170, Taiwan

* Correspondence: jchsieh@ncut.edu.tw

Received: 2 July 2025; Revised: 11 August 2025; Accepted: 4 September 2025; Published: 16 September 2025

Abstract: The present study provides a systematic review of expander technologies used in organic Rankine cycle (ORC) systems, examining their operational principles, performance characteristics, and application domains. Expanders can be broadly categorized into turbo and volumetric types, each exhibiting distinct operational advantages. Turbo expanders exhibit high isentropic efficiency and are well suited to high-temperature, high-mass-flow conditions. Their performance strongly depends on blade geometry and operating conditions, which can be optimized through computational fluid dynamics, meanline design, and advanced features such as variable guide vanes and partial admission. Volumetric expanders—including scroll, vane, and screw expanders—are commonly adopted in small- to medium-scale systems because of their simplicity, low cost, and ability to handle two-phase fluids. Scroll expanders are most effective at power outputs below 6 kW, whereas screw expanders provide a wider operational speed range and higher adaptability. Vane expanders, while compact, suffer from efficiency limitations due to internal leakage. All volumetric expanders face technical challenges related to sealing effectiveness, frictional losses, material selection, and thermal stresses. Turbo expanders, which require high manufacturing precision, are more frequently analyzed via simulations than experiments. This review consolidates current advancements, identifies unresolved technical barriers, and outlines strategies for performance enhancement. The insights presented herein are expected to inform expander selection, support system-level design (including control strategies for variable heat sources and mechanical expander–generator coupling), and guide future research, ultimately facilitating the deployment of ORC systems in sustainable and low-grade heat recovery applications.

Keywords: organic Rankine cycle (ORC); expander; isentropic efficiency; volumetric efficiency; low-grade heat; variable heat source

1. Introduction

As environmental problems have become increasingly severe, improving energy efficiency, reducing carbon emissions and developing green energy have become global priorities [1]. Consequently, the organic Rankine cycle (ORC) has increasingly been studied for its ability to efficiently convert low-grade heat into electricity. The ORC has been extensively applied in areas such as industrial waste heat recovery, geothermal energy, biomass utilization, and solar power generation [2]. Figure 1 illustrates the trends in installed capacity from 1984 to 2016 across four major application areas: biomass, geothermal, waste heat recovery, and solar. The West Texas Intermediate crude oil price is included as a reference indicator to investigate the potential correlation between global energy prices and the annual installed capacity of these applications. The final label on the timeline, "I.C." (in construction), represents projects that are currently under development. By the end of 2020, the global cumulative ORC installed capacity reached 4.07 GW, a 40% increase since 2016, with geothermal capacity contributing most to this change. Although the COVID-19 pandemic led to many challenges in this field, most manufacturers remain optimistic regarding the market's development in the short term and predict that Central and Eastern Europe and Southeast Asia will be the regions with the greatest growth potential. Additionally, geothermal and small waste heat sources are the most promising green sources under development [3]. ORC technology converts low-grade heat into electricity and represents a substantial advance in the energy sector. The ORC functions similarly to the traditional Rankine cycle (RC), with the primary distinction being the working fluid employed. RC systems use water as the working fluid and are suitable for high-temperature sources because water has a high saturation temperature. Notably, under heat source conditions below 300 °C, RC system conversion efficiency is reduced. Furthermore, during the expansion process, vapor tends to condense, and the resulting liquid droplets can strike turbine blades at high velocities, potentially reducing the lifespan of the expander. For these reasons, RC systems are primarily used in high-temperature applications such as coal-fired and nuclear power plants. By contrast, ORC systems employ organic fluids with low boiling points that undergo phase changes at lower temperatures, with these fluids including R245fa, R134a, hydrocarbons, toluene, and isopentane. The low boiling points of these fluids facilitate energy conversion from low-temperature heat sources, rendering ORC particularly well-suited for applications such as geothermal energy and industrial waste heat recovery.

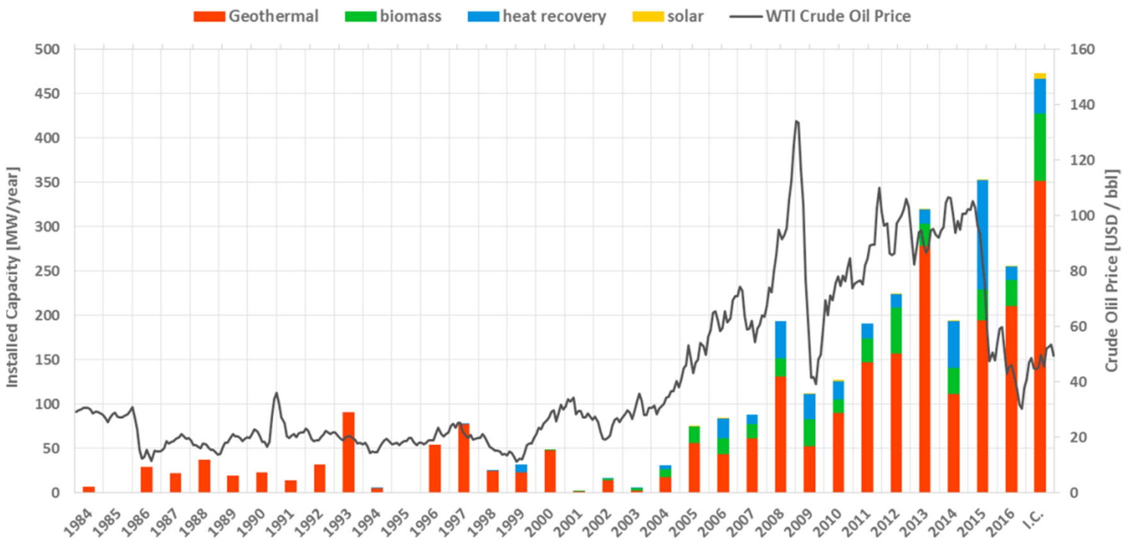

Figure 1. Evolution of installed capacity over time by application. Reprinted with permission from Ref. [4].

The economics of ORC systems are shaped by a complex interplay of technical, environmental, and financial factors. This section outlines the key limitations and challenges that affect both the performance and cost-effectiveness of ORC systems, particularly in small- to medium-scale applications.

1. Efficiency constraints and working fluid limitations

The thermal efficiency of ORC systems is generally lower than that of conventional RC systems, because of the smaller temperature differential between the heat source and ambient temperature, which limits the attainable Carnot efficiency. Additional inefficiencies arise from irreversible losses in the evaporator and condenser and from internal leakage and friction losses within the expander. The selection of an appropriate working fluid is therefore critical and must account for multiple criteria, specifically, low global warming potential (GWP) and ozone depletion potential, safety, favorable thermodynamic properties, dry or isentropic behavior, and suitable evaporation pressure [5,6].

2. Capital investment and operating costs

ORC systems require substantial initial capital investment, primarily because of the high costs of key components such as heat exchangers and expanders. This cost burden is particularly pronounced for small-scale systems, in which the levelized cost of electricity is high, and this limits these systems' economic feasibility. Moreover, many industrial applications require heat recovery units specifically designed for particular heat sources, which further increases upfront expenditure [7]. Additionally, environmentally benign working fluids are often costly, and their periodic replenishment—combined with system maintenance requirements—contributes substantially to long-term operational expenses.

3. Environmental influence of working fluid

The environmental footprint of ORC systems is strongly influenced by the choice of working fluid. Hydrofluorocarbons, such as R134a and R245fa, have been extensively adopted because of their favorable thermophysical properties. However, their high GWP has led to increasing regulatory restrictions and a shift toward low-GWP alternatives. Hydrofluoroolefins have emerged as promising replacements alongside natural fluids such as hydrocarbons. Nevertheless, these alternatives are associated with challenges, such as flammability risks, safety concerns, and potential compatibility problems with system materials [8].

4. Technical challenges of expanders

Volumetric expanders are commonly used in small- and medium-scale ORC systems, whereas turbo expanders are preferred in larger-scale applications. Although advancements have been made in these technologies, several challenges pertaining to internal leakage, frictional loss, thermal expansion and contraction, and optimal material selection remain [9]. Furthermore, the performance of expanders tends to deteriorate under fluctuating heat source and cooling conditions, reducing system reliability and efficiency.

5. Condensation and heat rejection problems

Effective heat rejection is essential to maintaining low condensation pressure and ensuring stable ORC operation. However, while water-cooled condensers are limited by the availability of cooling water, air-cooled condensers exhibit lower heat transfer performance. Consequently, system efficiency may decline substantially under high ambient temperature conditions, particularly during the summer [10].

ORC expanders convert the thermal energy of the working fluid into mechanical power, which drives a generator to produce electricity. As the core component of the ORC system, the expander is a key determiner of system efficiency, reliability, and economic viability [5]. Expanders can be divided into turbo expanders and volumetric expanders, depending on their operating conditions and power capacity. Turbo expanders, such as turbines, rely on high-speed fluid flow to drive rotor blades. They convert the fluid's kinetic energy into mechanical work. These expanders operate at tens of thousands of revolutions per minute and are suitable for large-scale systems with high rates of mass flow of the working fluid [11]. Turbo expanders are extensively used in geothermal power plants and commercial renewable energy systems. The advantages of turbo expanders include high efficiency and low operating noise. However, they require high levels of precision in manufacturing, advanced lubrication technologies, and complex aerodynamic designs. By contrast, volumetric expanders convert energy through the periodic expansion and contraction of enclosed chambers. They are superior under low-flow, low-speed, and high-pressure-ratio working fluid conditions [12]. Scroll, screw, vane, and piston expanders are among the most commonly used types of volumetric expanders. Although their peak efficiency is typically lower than that of turbo expanders, volumetric expanders exhibit stable performance under off-design conditions, rendering them advantageous for small- to medium-scale ORC systems such as those used in biomass power generation, solar thermal conversion, and waste heat recovery. Additionally, volumetric expanders have simpler mechanical structures and lower maintenance costs. However, their output power and isentropic efficiency are lower than those of turbo expanders, and their isentropic efficiency is affected by friction and internal leakage losses. Therefore, further research on expander design, operation characteristics, and technological trends is crucial to identifying the most appropriate expander for specific ORC applications.

2. Introduction of Turbo Expanders

Turbo expanders are extensively used in low-grade heat recovery applications because of their high efficiency and adaptability to medium- and large-scale systems. Turbo expanders function on the basis of the thermodynamic process of near-isentropic expansion. As the high-pressure, high-temperature working fluid expands through the turbine, its pressure and thermal energy are converted into kinetic energy. The stator guides and accelerates the flow, and the rotor extracts the flow's kinetic energy and converts it into mechanical power.

As the working fluid enters a turbo expander, it first passes through a stator, which acts as a nozzle, accelerating the movement of the fluid and enabling nearly isentropic expansion. This process considerably increases the fluid velocity, which often reaches sonic or supersonic speeds. The high-speed fluid strikes the rotor blades at a specified angle, transferring momentum and driving the rotor. At this stage, the fluid expands further, causing a rapid drop in temperature and pressure. The kinetic energy of the moving fluid is converted into mechanical energy, which is used to drive a generator and produce electricity. After the expansion process, the fluid exits the turbo expander at a lower pressure and enthalpy. Although the process ideally involves isentropic expansion, efficiency losses often occur in practical operation due to factors such as friction and internal leakage [13].

Turbo expanders can be classified as radial or axial on the basis of the direction of fluid flow. Each type of turbo expander has distinct advantages, with suitability determined by system requirements. Selecting an appropriate turbo expander design requires evaluating the inlet and outlet conditions of the expander, such as pressure, temperature, and mass flow rate. Engineers must also determine key design parameters, such as the flow coefficient, load coefficient, and reaction degree, to calculate the turbine's specific speed. In design charts (e.g., Figure 2), the specific speed supports the preliminary selection of a suitable turbo expander on the basis of the requirements of an ORC system.

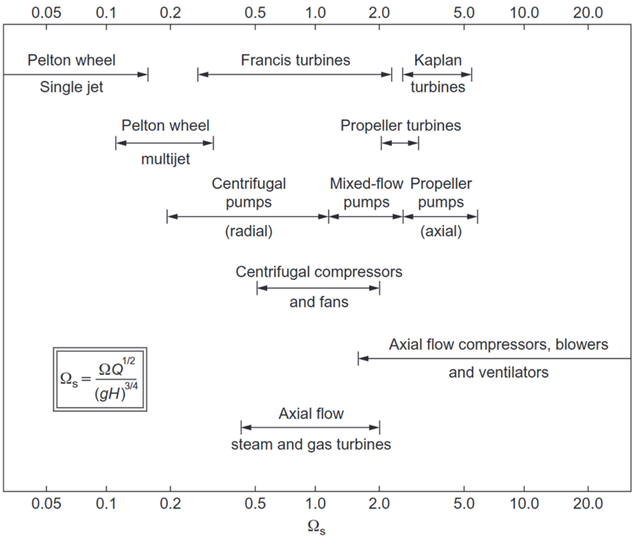

Figure 2. Range of the specific speeds for various types of turbo expander. Reprinted with permission from Ref. [14].

From an aerodynamic perspective, the performance of turbo expanders is highly dependent on airfoil and the thermophysical properties of the working fluid. The blade profile and fluid flow properties directly affect energy conversion efficiency, and specific heat capacity, density, and molecular weight affect the fluid's behavior at high velocities. Additionally, a turbo expander's isentropic efficiency is linked to parameters such as pressure ratio, mass flow rate, and rotation speed, which require the application of analytical approaches using theoretical methods such as the Euler turbine equation [14]. In ORC applications, organic working fluids typically have a low speed of sound and a high molecular weight [15]. Therefore, the design of turbo expanders must be optimized using real-gas properties to ensure stable and effective operation under specific thermodynamic conditions [16].

2.1. Turbo Expanders

2.1.1. Radial Turbo Expander

Radial turbine geometry typically involves the use of the CFturbo software or meanline design method ([16,17]) to facilitate the determination of geometric parameters such as blade angles and rotor dimensions during the preliminary design phase. These methods ensure optimal flow field and efficiency under the design conditions. To minimize kinetic energy losses caused by transonic or supersonic flow, the Mach number at the stator outlet should be maintained at 0.9 [18]. Additionally, the clearance between the blade tips and the casing should be minimized because excessive gaps can lead to internal leakage and flow separation, adversely affecting turbine performance [19].

The working fluid in a radial turbo expander flows radially with respect to the rotor axis, a characteristic that renders it particularly well-suited for applications involving low mass flow rates and high pressure ratios. Compared with axial turbo expanders, radial turbines offer advantages including a smaller size, higher efficiency, and lower manufacturing costs [15]. Table 1 presents the key parameters of radial turbines and indicates that R245fa is the most commonly used working fluid in such devices, with rotation speeds typically ranging from 10,000 to 60,000 rpm with a maximum output power of 712.03 kW.

Many low-grade heat sources, such as solar energy, geothermal, and industrial waste heat, exhibit fluctuations and intermittency, as illustrated in Figure 3, and ORC systems operate under off-design conditions. Hence, the control strategy for the turbo expander is critical to system efficiency. Currently, for heat sources with such fluctuations, radial turbo expanders are designed using compensatory control strategies, including sliding-pressure control and constant-pressure control. When the heat source supply is limited, constant-pressure control with variable inlet guide vanes can be applied to ensure that the turbine maintains efficiency under low mass flow conditions. By contrast, when the heat source supply is sufficient, sliding-pressure control is superior in enhancing the system's power output [17].

Table 1. Operational parameters and performance of radial turbo expanders in the literature.

Refs.	Methods	$T_{exp,in}$(°C)	Working Fluid	η_{exp}^{is}(%)	$W_{shaft/elec}$(kW)	rpm
Sauret et al. [16]	CFD	140	R134a	83.5	421.5	24,250
Dong et al. [20]	CFD	300	MM	80.4	180.6	30,000
Zheng et al. [13]	CFD	82.58	R134a	84.3	669.9	8000
Kim et al. [21]	CFD	N/A	NOVEC649	79.8	13.98	20,000
Du et al. [22]	CFD	N/A	R245fa	84.39	154.93	7800
Xia et al. [23]	CFD	140	R143a	83.24	419.23	25,160
Quan et al. [24]	CFD	80.17	R245fa	77.93	712.03	4778
Sarmiento et al. [25]	CFD	89.54	R245fa	90.24	13.98	8000
Yao et al. [19]	CFD	85	R245fa	84.67	9.016	52,335
Li et al. [26]	CFD	100	R245fa	91.7	N/A	39,220

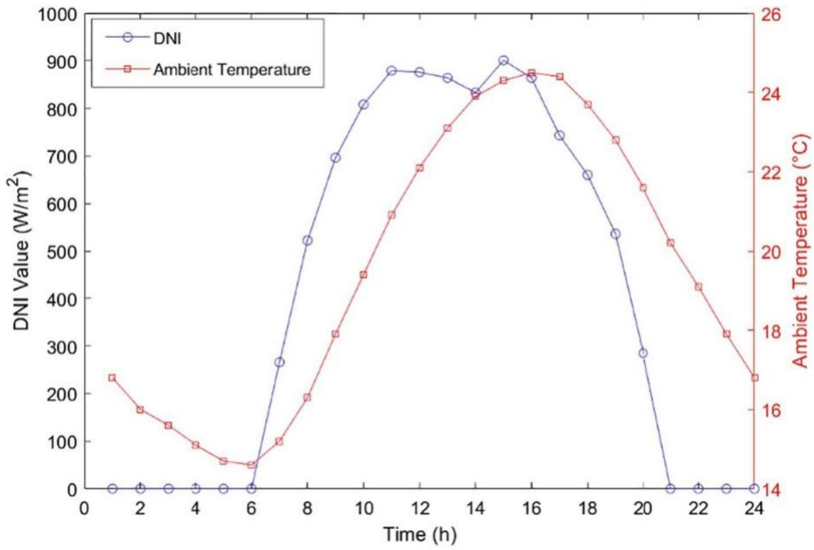

Figure 3. Associations of direct normal irradiance and ambient temperature with time. Reprinted with permission from Ref. [27].

2.1.2. Axial Turbo Expanders

The design of the geometric parameters for axial turbines is based on CFturbo and the meanline design method [28]. The literature recommends using a lower reaction degree to reduce blade loading and the required rotor rotation speed. A lower rotation speed can reduce vibrations caused by high-speed rotation, extending the turbo expander's operational lifespan [28]. Axial turbo expanders operate with the working fluid flowing parallel to the rotor shaft, rendering them suitable for conditions involving high mass flow rates and low pressure ratios. Because single-stage turbo expanders typically have low pressure ratios, a multistage configuration can be used to increase the overall pressure ratio and address the limitations of single-stage designs [29]. The use of a multistage configuration enables axial turbo expanders to meet higher power demands. Additionally, because of their high output capacity, multistage configurations are especially well-suited to commercial applications, such as geothermal power plant. Compared with radial turbines, axial turbo expanders offer higher power output and are superior under high-flow conditions; however, they tend to be larger and more complex to manufacture. Table 2 presents the key parameters of axial turbo expanders in the literature. In axial turbo expanders, R245fa is the most commonly used working fluid, with rotation speeds typically ranging from 10,000 to 30,000 rpm and a maximum power output of 1720 kW.

Table 2. Operational parameters and performance of axial turbo expanders in the literature.

Refs.	Methods	$T_{exp,in}$ (°C)	Working Fluid	η_{exp}^{is}(%)	$W_{shaft/elec}$(kW)	rpm
Witanowki et al. [30]	CFD	87	R245fa	78.91	13.05	18,000–20,000
Yang et al. [31]	EXP	84	R245fa	78.52	163.44	1500
Sun et al. [32]	CFD	226.96	MM	82.7	140	N/A
Jubori et al. [33]	CFD	120	R245fa	46.3 (PDC)	18.21	10,000
Peng et al. [34]	CFD	200	MM	77.46	83.80	15,000
Sun et al. [35]	CFD	112	R245fa/R134a	86.4	1720	11,374
Naas et al. [36]	CFD	92	n-pentane	88.03	12.95	16,000

Table 2. *Cont.*

Refs.	Methods	$T_{exp,in}$ (°C)	Working Fluid	η_{exp}^{is}(%)	$W_{shaft/elec}$(kW)	rpm
Klun et al. [37]	CFD	N/A	isopentane	74.8 (PDC)	60.35	9000
Alshammari et al. [38]	CFD	120	R245fa	55.3 (PDC)	9.95	20,000
Kupka et al. [28]	CFD	105	R1233zd(E)	84	18.24	27,000

In many application scenarios, such as waste heat recovery and geothermal power generation, heat sources exhibit fluctuations and intermittency. Therefore, axial turbo expanders are required to operate under off-design conditions, rendering off-design control strategies crucial. The control strategy for axial turbo expanders involves partial admission control. When the heat source supply is insufficient and the mass flow rate is low, the effective flow area is adjusted to enhance control of output power and maintain efficiency [39], as illustrated in Figure 4.

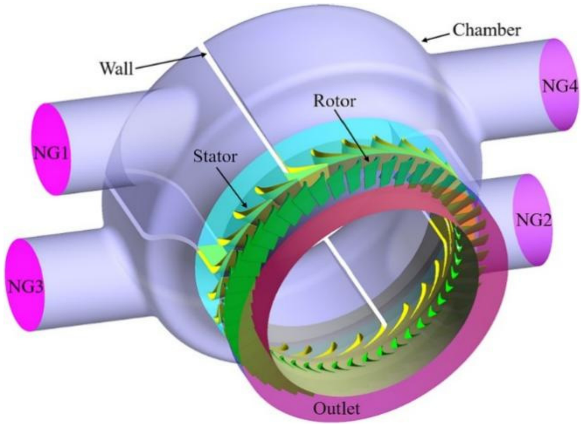

Figure 4. Schematic of partial admission. Reprinted with permission from Ref. [40].

2.2. Volumetric Expanders

Compared with turbo expanders, volumetric expanders (positive-displacement expanders) have a lower cost and simpler internal structure. They also have several operational advantages, such as tolerance for higher pressure ratios, lower rotation speeds, and the ability to operate with two-phase flows [41]. Their small size renders them particularly suitable for space-constrained applications such as small-scale ORC systems, waste heat recovery from automobile engines, and distributed power generation systems [13]. In volumetric expanders, the working fluid pressure is gradually reduced through an increase in the internal chamber volume along the direction of flow. The volumetric ratio of the expander is calculated as the ratio of the expansion chamber's final volume to its initial volume during the expansion process. This inbuilt volumetric ratio is a key parameter influencing the efficiency of volumetric expanders. The ratio is determined by the geometry and flow characteristics of the machine, and the actual expansion ratio depends on operating conditions such as the evaporation and condensation pressures of the working fluid [42]. A mismatch between the inbuilt and actual expansion ratios can lead to substantial losses in isentropic efficiency. In practice, under-expansion is typically preferable to over-expansion, especially when system efficiency and machine size are considered [43]. Over the past decade, extensive research has been conducted on the performance of volumetric expanders for small-scale low-grade heat recovery systems. Most such expanders have been adapted from compressors and modified through reverse operation and redesign to function effectively as expanders. Volumetric expanders may be vane, screw, piston, or scroll expanders, each of which have unique application domains and performance. Although compressor technology is well-established and extensively commercialized [44,45], most small-scale ORC systems currently use modified compressors as expanders because the market for volumetric expanders is in its infancy. Currently, only a few types of volumetric expander—such as scroll and screw expanders—are available commercially [46,47]. Selecting an appropriate expander for low-grade heat applications requires comprehensive consideration of overall dimensions and weight, lubrication, feasibility, reliability, and coupling with electric generators [48]. In response to these considerations, various volumetric expanders have been investigated for low-grade heat applications, with their performance evaluated through different modeling approaches and computational fluid dynamics (CFD) techniques [21,49].

2.2.1. Scroll Expanders

The scroll expander is one of the most extensively used volumetric expanders in ORC systems because of its simple structure, compact size, and high efficiency. Additionally, scroll compressors are widely available and have similar mechanical designs, rendering them a practical basis for experimental studies that develop scroll expanders by modifying scroll compressors. As illustrated in Figure 5, the components of a scroll expander are two interleaved spiral scrolls. Scroll expanders operate in three steps: suction (I), expansion (II and III), and discharge (IV). The core structure contains fixed and an orbiting scroll that move along an eccentric path. During operation, high-pressure gas enters the central chamber of the expander and is drawn into the internal pockets formed between the scrolls as the orbiting scroll rotates. As the orbiting scroll moves, the volume of these gas pockets gradually increases, leading to a decrease in pressure and enabling the gas to expand and perform work. The expanded gas is pushed outward along the scroll path and eventually discharged through an outlet at the periphery of the expander. Throughout the process, the orbiting scroll follows a counterclockwise trajectory, enabling the outward expansion and energy release of the working fluid.

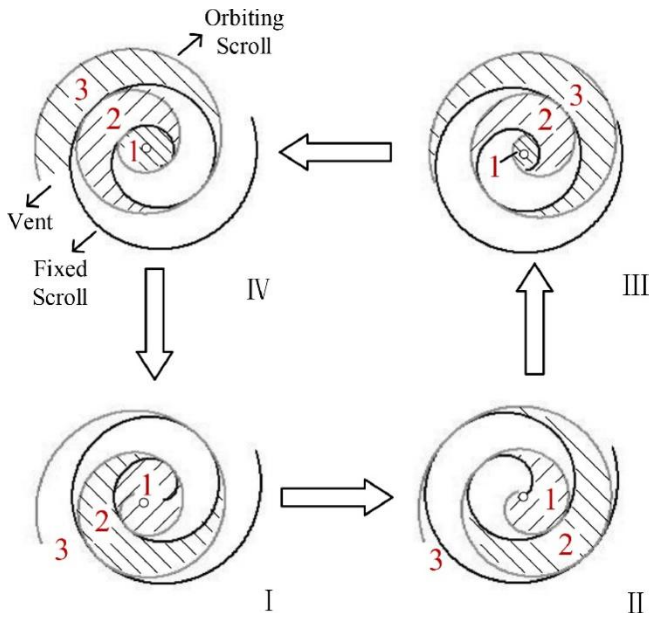

Figure 5. Operational principles of scroll expanders. Reprinted with permission from Ref. [50].

As early as 1988, Yanagisawa et al. [51] demonstrated the feasibility of using scroll expanders for low-grade heat applications by modifying an automotive air-conditioning compressor into a scroll expander. Their experiments, conducted within a rotation speed range of 1000 to 4000 rpm, achieved isentropic efficiencies between 60% and 75%. Hsieh et al. [52,53] have improved the range of the heat transfer rate and isentropic efficiency of the system by adjusting the rotation speed and operation mode of a scroll expander modified from a vehicle air-conditioning compressor. Their modifications increased the isentropic efficiency from 47.3% to 65.8%. They also reported that the isentropic efficiency of the scroll expander decreased with an increase in rotation speed, with the optimal performance observed at 1350 rpm. The performance of scroll expanders can also be increased by optimizing the end involute angle, which enhances both average output power and output stability [54]. Additionally, enclosing an open-drive scroll expander within a sealed steel shell and using magnetic coupling for power transmission effectively mitigates leakage and preserves system integrity [49]. With advances in ORC heat recovery technologies—particularly micro- and small-scale systems—numerous studies have focused on the design and optimization of scroll expanders, employing various methods in simulations and experimental analysis. Most studies have reported the measured performance of scroll expanders under experimental conditions, with isentropic efficiency values ranging from 25% to 80%. Table 3 presents the key parameters of scroll expanders and indicates that R245fa is the most commonly used working fluid in ORC systems. The typical rotation speed for scroll expanders ranges from 500 to 4000 rpm; however, depending on the application, rotation speeds can be as low as 1000 rpm and as high as 8000 rpm, with a maximum power output of approximately 6 kW. Although scroll expanders produce less power output than turbo expanders do, they have simple structures and are suitable for small-scale ORC systems.

Table 3. Operational parameters and performance of radial scroll expanders in the literature.

Refs.	Methods	$T_{exp,in}$(°C)	Working Fluid	η_{exp}^{is}(%)	$W_{shaft/elec}$(kW)	rpm
Hsieh et al. [52]	Exp.	N/A	R134a	65.8	2.05	1800
Fukuta et al. [55]	Exp.	40	S-CO_2	80	N/A	2000–4000
Declaye et al. [49]	Exp.	N/A	R245fa	75.7	2.1	3500
Gao et al. [56]	Num.	N/A	R134a	70	3.435	1140
Kosmadakis et al. [57]	Exp.	N/A	R404a	40	1.4	580
Cambi et al. [58]	Exp./Num.	50	R410A	50	N/A	N/A
Giuffrida et al. [59]	The.	111.5	R1234ze(Z)	64	2	2800
Yang et al. [60]	Exp.	100	R1233zd(E)	69	0.475	950–1550
Dumont et al. [61]	Exp.	122-133	R245fa	76	1.544	1137–7920
Ziviani et al. [62]	Exp.	110	R245fa	58	3.75	2500
Fatigati et al. [63]	Exp.	N/A	R245fa	55	0.65	1000–4000
Hijriawan et al. [64]	Exp.	90	R134a	74	2.292	505.8
Wang et al. [65]	Exp.	N/A	R245fa	50–58	0.831	2700–3300
Zhang et al. [66]	Exp.	95	R245fa	74.8	1.73	1500–2437
Feng et al. [67]	Exp.	106.5	R245fa	25–68	6	N/A
Zhen et al. [68]	Exp./Num.	130	R245fa	49.4	3.053	2000

Exp: Experiment. Num: numerical.

2.2.2. Piston Expanders

The piston expander offers several advantages in ORC systems, such as a simple structure, suitability for intermittent operation, and the ability to accommodate large pressure variations. However, the literature on piston expanders remains limited, and the designs of such expanders vary widely. The operational principle of a piston expander is similar to that of an internal combustion engine, with the key difference being that the energy source is the expansion of a high-pressure working fluid rather than fuel combustion. In an ORC system, the working fluid is first heated by an external heat source and vaporized into a high-temperature, high-pressure gas that enters the cylinder of the piston expander. As the working fluid expands and drives the piston, its thermal energy is converted into mechanical energy, which rotates the crankshaft and can subsequently power a generator or other mechanical loads. After expansion, the working fluid is discharged from the cylinder, condensed in a condenser, and returned to the cycle. A common type of piston expander is the reciprocating expander, the components and structure of which are illustrated in Figure 6.

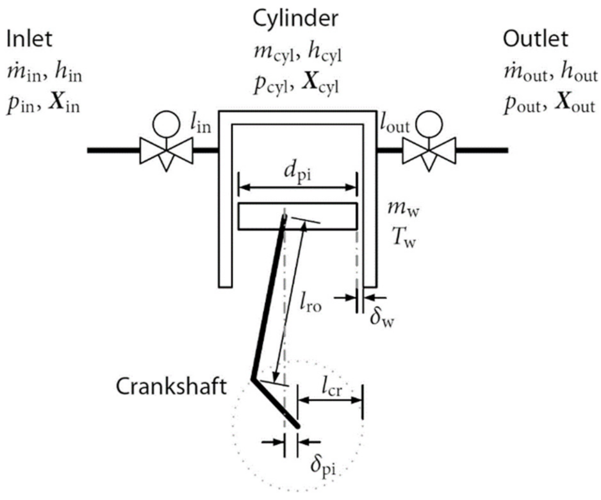

Figure 6. Components and structure of a reciprocating piston expander. Reprinted with permission from Ref. [69].

Piston expanders are classified as single-acting and double-acting. A single-acting expander completes one expansion stroke per cycle, whereas a double-acting expander achieves two expansion strokes within a single cycle. Research on piston expanders has focused on several key configurations, such as reciprocating piston, radial piston, rolling piston, and StarEngine piston expanders. Table 4 presents a summary of the literature on various types of piston expanders, highlighting how their structural design considerably influences performance. The isentropic efficiency of piston expanders in ORC systems is substantially affected by rotation speed, friction, leakage, and working fluid properties. Higher rotation speeds can improve volumetric efficiency by reducing leakage time, but excessive speeds increase mechanical losses due to friction and wear. Oudkerk et al. [70]

conducted experimental tests on a 195-cm^3 swash-plate piston expander integrated into an ORC system, with R245fa used as the working fluid. The results revealed that at the optimal operating speed of 2500 rpm, most losses were attributable to under-expansion and recompression, followed by mechanical losses, leakage, and pressure drop in descending order of magnitude. Friction losses from piston–cylinder contact are a major energy drain, especially in oil-free designs, and must be addressed using optimized materials and lubrication strategies. Leakage through piston–cylinder gaps also reduces efficiency but can be mitigated through precise geometry and sealing.

Table 4. Operational parameters and performance of radial piston expanders in the literature.

Refs.	Types/Methods	$T_{exp,in}$ (°C)	Working Fluid	η_{exp}^{is} (%)	$W_{shaft/elec}$(kW)	rpm
Zheng et al. [71]	Rolling piston /Exp.	76.5–87.7	R245fa	43.3	0.35	350–800
Han et al. [72]	FPC/Num.	100	R245ca	44.3	N/A	50
Wronski et al. [69]	Reciprocating Piston/Exp./Num.	125	N/A	70	2.5	N/A
Chatzopoulou et al. [73]	Piston/Num.	N/A	R1233zd	82	100	1500
Bianchi et al. [74]	StarEngine piston/Exp.	84.5	R134a	43	0.25–1.15	320–1100
Bianchi et al. [75]	Reciprocating Piston/Num.	65–85	N/A	40	0.3–1.4	320–900
Bianchi et al. [76]	Reciprocating Piston/Num.	75	R134a	36	0.943	832
Han et al. [77]	Radial piston	152.8	R245fa	64.8	0.279	90–1650
Gao et al. [78]	Opposed rotary Piston/Num.	180	Air	68	11	500–1500

Exp: Experiment. Num: numerical.

2.2.3. Screw Expanders

Screw expanders such as the twin screw expander (TSE) consist of a casing, female rotor, male rotor, synchronization gears, bearings, and sealing elements, as illustrated in Figure 7. Because they use a pair of rotors, TSEs balance forces and ensure stable operation, rendering them well-suited to high-pressure, high-temperature, and large-flow applications in ORC systems, such as those for waste heat recovery in the steel and chemical industries.

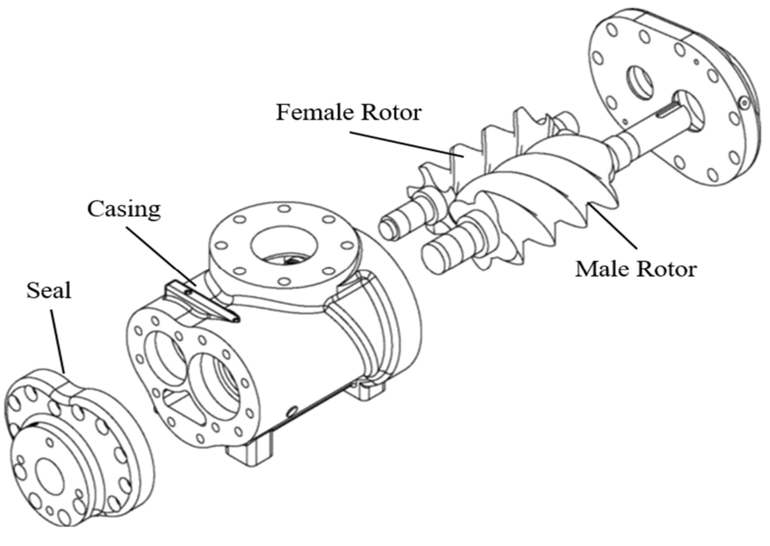

Figure 7. Structure diagram of a TSE. Reprinted with permission from Ref. [12].

The operational principles of a screw expander are illustrated in Figure 8. The expander operates through meshing of the male and female rotors, completing the processes of intake, expansion, and exhaust and converting the internal energy of the working fluid into mechanical energy. High-pressure vapor from the working fluid enters the V-shaped working chamber (A). As the rotors rotate, the vapor gradually moves into chambers B and C, where its volume expands and drives the rotor. Finally, the gas reaches chamber D and is discharged through the exhaust port.

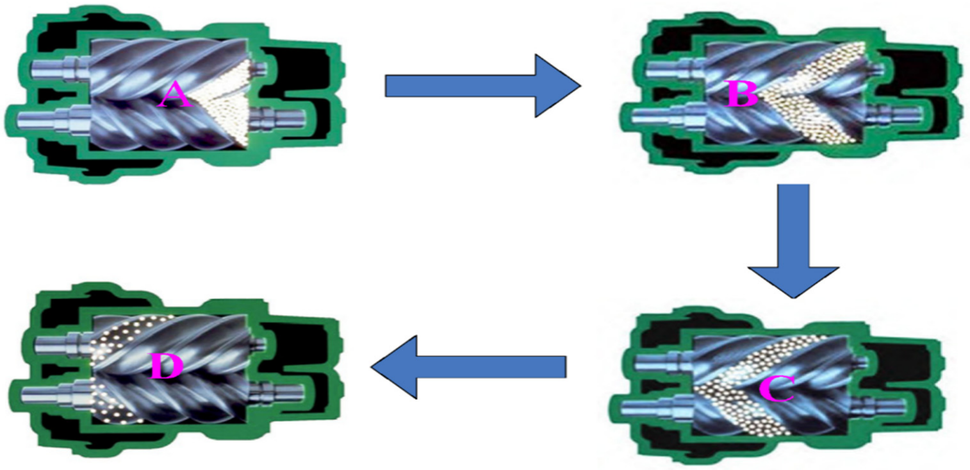

Figure 8. Diagram of the operational principles of a TSE. Reprinted with permission from Ref. [79].

A single-screw expander (SSE) consists of a 6-groove screw, two 11-tooth star wheels, and a casing, as illustrated in Figure 9. The two star wheels are symmetrically positioned on both sides of the screw, ensuring balanced radial and axial forces. Through the alternating meshing of the grooves and teeth, the expander facilitates the transport of the working fluid from intake to exhaust, delivering power through an extended shaft. Compared with TSEs, SSEs have lower leakage rates and higher volumetric efficiency, rendering them particularly suitable for low-grade and small-scale system applications.

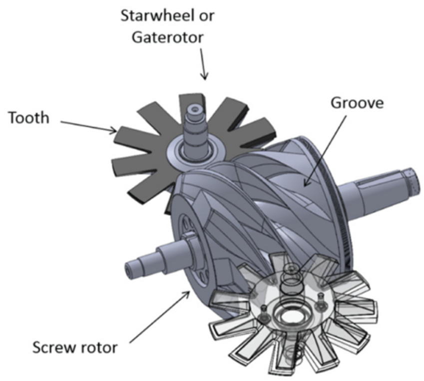

Figure 9. Structural diagram of an SSE. Reprinted with permission from Ref. [80].

The operational principles of an SSE involve high-pressure working fluid entering the working chamber formed between the screw and the star wheels. As the screw rotates, the chamber expands, completing the intake process. The gas undergoes expansion, driving the rotation of the screw and converting energy and reducing pressure. Finally, the low-pressure gas is discharged through the exhaust port. The sealing components of the screw expander are critical, directly affecting its performance and operational reliability.

Similar to other volumetric expanders, screw expanders are subject to challenges such as internal leakage and frictional losses that can adversely affect their overall performance and efficiency. Studies have demonstrated that increasing rotation speed can extend the steam flow path through wall-drag effects, reducing shaft seal leakage. Additionally, higher inlet mass flow rates considerably increase expander performance [81,82]. Optimizing the clearance between the rotor and casing and between the screw and casing can also enhance the performance of SSEs [83,84]. The efficiency of screw expanders tends to increase with the pressure ratio and reaches its maximum at high rotation speeds; additionally, an increase in steam quality at the inlet markedly enhances the torque and output power of SSEs [85].

In terms of tooth profile design, a multicolumn (or multiline) approach enables the contact line between the tooth and groove flanks to move across the entire tooth flank area, increasing lubrication and extending service life [86]. Moreover, adjusting the length of the intake manifold can effectively mitigate the adverse effects of inlet expansion on system performance [87].

Regarding the discharge process of steam within the screw grooves, studies have indicated that discharged steam can be converted into additional power. Through exhaust kinetic energy utilization, under-expansion losses can be effectively reduced, with particularly substantial benefits observed in large-scale units [88]. Furthermore, the kinematic viscosity of lubricants has a notable influence on shaft efficiency and gas consumption at low rotation speeds. Selecting lubricants with appropriate viscosity that are tailored to different inbuilt volume ratios and clearances is also crucial to enhancing overall performance [89].

Table 5 summarizes the literature on SSEs and TSEs, providing a comparison of their rotation speed ranges and working fluid choices. SSEs operate within a speed range of approximately 1233–3200 rpm, rendering them suitable for medium- and small-scale applications. SSEs have a simple structure, stable operation, and low vibration and noise. By contrast, TSEs have a broader speed range of 1250–20,000 rpm, indicating greater adaptability, especially for high-speed and high-power-output applications. TSEs have superior durability and efficiency to those of scroll and piston expanders. Additionally, the higher rotation speed and wider speed range of TSEs provide exceptional flexibility in waste heat recovery, rendering them adaptable to various operating conditions.

Table 5. Operational parameters and performance of screw expanders in the literature.

Refs.	Methods	$T_{exp,in}$ (°C)	Refrigerant	η_{exp}^{is} (%)	$W_{shaft/elec}$(kW)	rpm
Zhang et al. [90]	Single/Exp.	123.62–140.26	R123	N/A	7.81–10.38	1233–1538
Hsu et al. [91]	Twin/Exp.	101	R245fa	72.4	50	3610-3670
Yang et al. [89]	Single/Exp.	114	R245fa	65	308.6	3200
Tang et al. [82]	Twin/Exp.	N/A	R123	60–88	N/A	1250–6000
Lei et al. [83]	Single/Exp.	N/A	R123	73	8.35	3000
Ziviani et al. [92]	Single/Exp.	125	SES36, R245fa	64.7	6.8–7.4	2000–3000
Ziviani et al. [93]	Single/Exp.	120	R245fa	N/A	8.5	2200
Nikolov et al. [94]	Twin/Exp.	110–130	R245fa	67	4	20,000
Dumont et al. [61]	Twin/Exp.	75–130	R245fa	30–55	1.29	500–12,450
Eyerer et al. [95]	Twin/Exp.	106–120	R245fa	80	330	2700–3300
Guo et al. [96]	Single/Exp.	110–140	R123, HFO-1336mzz(Z)	N/A	7.32	3000
Zhao et al. [97]	Twin/Exp.	255–265	steam	66.81–74.25	279–432	3687–3690
Wang et al. [98]	Single	159.6	R123	N/A	6.05	3000

2.2.4. Rotary Vane Expanders

The structure of rotary vane expander (RVEs) consists of a stator, rotor, vanes, bearings, and a rotor, as illustrated in Figure 10. The operational principle of RVEs involves reliance on the presence of several radial (or inclined) slots on the rotor, each containing a rectangular vane. The vanes can slide freely within the slots and remain in close contact with the inner wall of the stator because of centrifugal force during rotation, forming independent working chambers. When the working chamber has a small volume, working fluid enters through the inlet. As the rotor rotates, the chamber volume gradually increases, enabling the fluid to expand. When the vanes reach the exhaust port, the expansion process concludes, and the fluid is discharged from the expander [99].

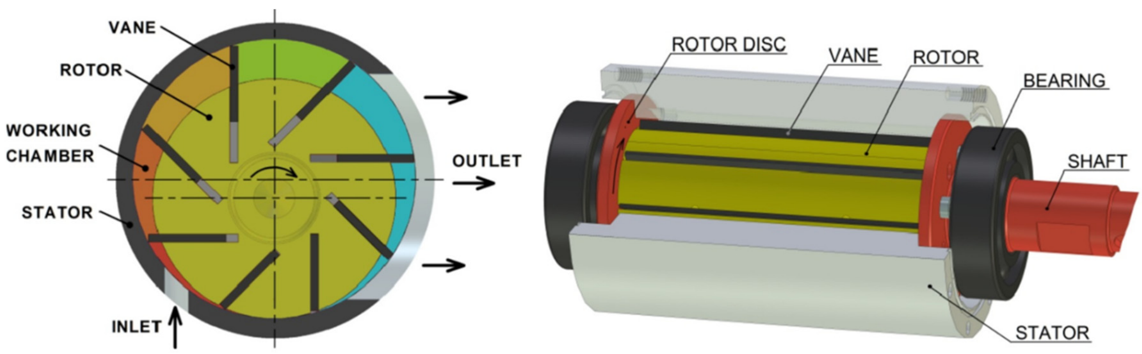

Figure 10. RVE structure diagram. Reprinted with permission from Ref. [99].

Leakage in RVEs is a major problem and is influenced by multiple factors, such as the pressure ratio, the number of leakage paths, the thermodynamic properties of the working fluid, and the proportion of lubricating oil in the working fluid [100]. Leakage has a considerable influence on the isentropic and volumetric efficiencies of the expander and may reduce the evaporation pressure, adversely affecting the overall system efficiency. RVEs can also be affected by vane flutter, in which the vanes fail to maintain stable contact with the stator inner wall surface. This instability can disrupt the filling process, leading to leakage between vanes and reducing the sealing performance between adjacent chambers. Such leakage can negatively affect the expander's filling factor and volume ratio. As illustrated in Figure 11, various leakage paths exist in RVEs [101]. The primary sources of leakage are as follows:

(1) Clearance between the stator and rotor end faces—Gaps at the end faces can enable working fluid to escape, reducing efficiency [102].

(2) Leakage between the vane tip and the stator inner wall—When the vane tip fails to maintain proper contact with the stator surface, leakage occurs, negatively affecting sealing performance [103].

(3) Leakage along the vane side edges—Gaps along the sides of the vanes can lead to fluid bypassing, reducing the effectiveness of the working chambers [104].

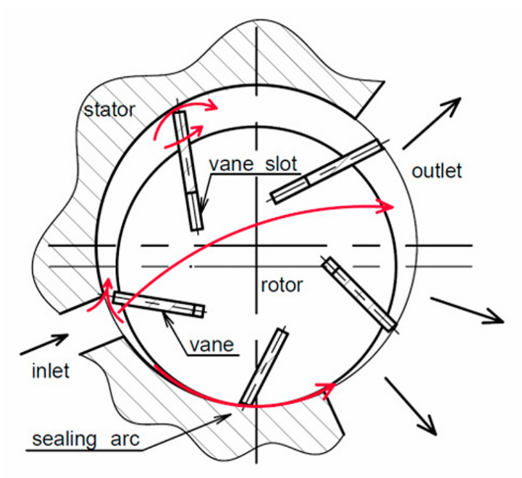

Figure 11. Primary leakage paths in RVEs. Reprinted with permission from Ref. [101].

Various technical approaches have been proposed to enhance sealing performance and reduce internal leakage in RVEs. Jia et al. [105] introduced springs placed beneath the vanes and within the vane slots, enabling the vanes to rapidly rebound and maintain tight contact with the cylinder wall, substantially increasing sealing effectiveness at the vane tips. Yang et al. [106] proposed using high-pressure gas at the rear side of the vanes to increase contact between the vanes and the cylinder wall and effectively mitigate leakage. Additionally, Casari et al. [107] investigated the characteristics of three-dimensional internal leakage flow fields and concluded that introducing lubricating oil can reduce leakage between the rotor and the housing. These studies provide valuable insights and design references for enhancing the sealing efficiency of RVEs.

Table 6 presents the key simulation and experimental parameters of the RVEs used in ORC systems. The table indicates that commonly used working fluids include MM, R134a, and R245fa. The inlet vapor temperature ranges from 42 °C to 192 °C, indicating the suitability of RVEs for low- to medium-temperature heat sources. The isentropic efficiency varies between 40% and 73%, and the output power ranges from 0.8 to 4.37 kW, depending on design and application conditions. Operating rotation speeds are primarily between 1850 and 3328 rpm, suggesting that RVEs are suitable for medium- to low-speed operation. Although their power output is lower than that of turbine expanders, RVEs are extensively applied in small-scale ORC systems because of their simple structure, rapid startup, and ease of maintenance.

Table 6. Operational parameters and performance of vane expanders in the literature.

Refs.	Methods	$T_{exp,in}$ (°C)	Refrigerant	η_{exp}^{is} (%)	$W_{shaft/elec}$ (kW)	rpm
Vodicka et al. [101]	Sim.	80	MM	72.7	4.37	3000
Mascuch et al. [108]	Exp.	192	MM	46	3.2	3328
Naseri et al. [109]	Exp.	42-63	R134a	42.5	1.34	1850
Fatigati et al. [110]	Exp.	N/A	R245fa	40–50	0.8	2000

3. Comparison and Selection of Expanders

The selection of an appropriate expander is governed by several critical factors, specifically, heat source temperature, rotation speed, power capacity, thermodynamic performance, and economic considerations. In the literature, scroll expanders are the most extensively studied volumetric expanders because of their suitability for small-scale power generation (<5 kW) and their high availability. Common working fluids used in scroll expanders include R123, R1233zd, R134a, and R245fa. Screw expanders offer a wide operational speed range and are capable of handling large amounts of waste heat; however, their performance is substantially inferior to that of turbo expanders. Screw expanders are typically applied in medium- to large-scale systems. Piston expanders are well-suited for applications with large pressure ratios. Despite their low rotation speed, they tend to produce higher noise levels. Vane expanders are also used in small-scale power generation (<5 kW); nevertheless, they experience greater leakage and friction losses, resulting in lower isentropic and volumetric efficiencies.

Radial turbines are the most commonly adopted configuration of turbo expanders. They are well-suited for medium-scale power generation (<1000 kW) and high-pressure-ratio applications, offering a favorable trade-off between efficiency and power output. By contrast, axial expanders are typically employed in large-scale systems (>1000 kW) with high mass flow rates. Their multistage designs enable high overall pressure ratios and can accommodate greater power demands, rendering them particularly suitable for commercial-scale geothermal power generation. A comparative summary of the various expander types applicable to ORC systems is presented in Table 7.

Turbo expanders typically operate at higher rotation speeds (>10,000 rpm), indicating stringent requirements with respect to the precision and durability of components such as bearings, seals, and rotating parts. Consequently, the design and manufacturing costs of turbo expanders are high. By contrast, volumetric expanders typically operate at lower rotation speeds and have less demanding requirements for component strength and precision, simplifying the design and manufacturing process and reducing costs.

Table 7. Performance comparison of expanders in ORC systems.

Types	$T_{exp,in}$ (°C)	$W_{shaft/elec}$ (kW)	rpm	Advantages	Disadvantages
Radial	80.17–300	9.016–712.03	4778–52,335	I. High efficiency II. Capable of high pressure ratios	I. High manufacturing cost II. Susceptible to choking at supersonic
Axial	84–226.96	9.95–163.44	1500–27,000	I. High efficiency II. Supports multi-stage configurations for high pressure ratios III. Handles high mass flow rates	I. High manufacturing cost II. Susceptible to choking at supersonic III. High rotation speed IV. Limited pressure ratio in single-stage application
Scroll	40–133	0.475–6	505.8–7920	I. Compact design II. Low noise	I. Leakage issues II. Have complicated geometry
Piston	65–180	0.25–100	50–1650	I. Suitable for larger pressure variations II. Operates at low rotation speeds III. Capable of high pressure ratios	I. High noise levels II. Very low power output capacity
Screw	75–265	1.29–432	500–20,000	I. Has a broader working range II. High volumetric efficiency	I. Complex manufacturing and sealing requirements II. High manufacturing cost
Vane	42–192	0.8–4.37	1850–3328	I. Simple mechanical structure	I. High leakage and friction losses II. Low volumetric efficiency

4. Expander Operation with Variable Heat Sources

ORC systems are extensively used to convert low-grade heat sources into electrical power, with typical sources including industrial waste heat, geothermal energy, and solar energy. The characteristics of these heat sources often fluctuate over time and under varying environmental conditions. For instance, industrial waste heat may vary with production schedules; solar energy is highly sensitive to weather and diurnal conditions; and for geothermal energy, the temperature and mass flow rate can be unstable because of variation in wellhead conditions [31]. These fluctuations may adversely affect overall system performance, particularly impacting the expander, which is a core component of the ORC system. Therefore, developing adaptive expander operation and control strategies has become essential.

Under variable heat source conditions, ORC systems commonly adjust the evaporation pressure to regulate the working fluid mass flow rate and external thermal load. Table 8 presents a summary of typical control strategies, along with their advantages and disadvantages. When the heat input decreases in the evaporator (e.g., the mass flow rate and temperature of the heat source decrease), the system must reduce the mass flow rate of the working fluid to prevent excessive thermal extraction. This is typically achieved by reducing the evaporation pressure. However, this adjustment lowers the expansion pressure ratio, which subsequently reduces the shaft power and isentropic efficiency of the turbo expander. This drop in performance is more pronounced under off-design conditions and indicates the limited tolerance of turbo expanders to load variation. Therefore, enhancing operational stability under variable heat source conditions has become a key challenge in ORC system design and control.

From the control perspective, pressure ratio adjustment is the main strategy employed in response to heat source fluctuations but is often supplemented by rotation speed control and partial admission to maintain the system's stability and efficiency. Despite these efforts, the controllable speed range of turbines is inherently limited, and the integration of variable inlet guide vanes (radial turbine) and partial admission control (axial turbine) can increase mechanical complexity and may cause aerodynamic instabilities and vibration problems, further limiting adaptability under dynamic loads. Although turbo expanders have relatively small turn-down ratios, they can be effectively utilized in specific applications in which the operational conditions are suitable. For example, they can be used in geothermal power plants and agricultural waste incineration systems, which typically operate in the hundred-kilowatt-to-megawatt scale. These power plants and incineration systems often have a relatively stable heat supply, which enables turbo expanders to operate close to their design conditions, thereby maintaining high efficiency.

In applications based on small and variable heat sources, such as industrial waste heat and solar collectors, specific challenges often arise in terms of maintaining stable turbine operation. In these scenarios, volumetric expanders are the better choice because they offer high flexibility and adaptability [111]. In Taiwan, Hanpower Energy Technology provides customized ORC systems that utilize induction generators. Compared with synchronous generators, induction generators are more cost-effective, require simpler control systems, and offer higher reliability, making them particularly suitable for small- and medium-scale ORC applications with fluctuating loads. Based on the ORC project list compiled from HanPower Energy Technology Co., Ltd. and summarized in Table 9, turbine-based systems are predominantly deployed in geothermal power plants, while twin-screw expander systems are mainly applied in industrial waste heat recovery, especially in installations with capacities below 300 kW.

In applications involving volumetric expanders, the ORC system primarily controls the pump variable frequency drive to adjust the evaporation pressure and working fluid mass flow rate, thereby regulating the expander's inlet conditions and ensuring adequate superheat. Because the isentropic efficiency of screw expanders varies with the pressure ratio, the control strategy must modify the evaporation pressure and mass flow rate on the basis of the real-time operating mode (e.g., overexpansion or underexpansion) [61]. In overexpansion scenarios, moderately increasing the evaporation pressure can improve efficiency. In underexpansion scenarios, the performance may degrade. These phenomena indicate that the operating conditions should closely align with the expander's built-in volume ratio and the corresponding optimal evaporation pressure. Additionally, adjusting the evaporation pressure serves as a mechanism for regulating the working fluid mass flow rate, ensuring it matches the heat absorbed from the heat source.

The method of coupling used between the expander and generator affects rotation speed, structural design, and control strategy implementation. The common mechanical coupling configurations include gearboxes, belt drives, and direct connections, each with specific technical limitations and suitable applications. Although high-speed turbo expanders offer excellent power density, their rotation speeds often exceed the rated speeds of induction generators. Therefore, gear reduction mechanisms are typically required for speed matching. For example, in a 250-kW ORC system, the speed of a 12,000-rpm turbine is reduced to 3600 rpm through a gearbox to drive an induction generator. Although this setup preserves the turbine's high-efficiency operation, it introduces additional mechanical loss, vibration, noise, and lubrication demands [112].

Volumetric expanders, such as screw and scroll expanders, which operate at low rotation speeds, are suitable for direct and belt-driven coupling. Belt transmissions offer mechanical flexibility and structural simplicity, and they achieve speed matching by adjusting pulley diameter ratios [52]. This setup enables variable-speed ORC configurations that ensure adaptability to variable heat source conditions and improve overall system performance. However, once the pulley ratio has been fixed (defined as the diameter of the generator pulley divided by that of the expander), the expander's rotation speed becomes mechanically constrained. Therefore, to change the expander's rotation speed, the pulleys must be manually disassembled and replaced, which limits the system's capability for real-time speed control. When belt-driven expanders are paired with induction generators, their rotation speed is restricted by the grid frequency, which makes them appropriate for applications involving stable heat sources and grid-connected operation. By contrast, permanent magnet generators enable off-grid operation and can regulate torque indirectly through electrical load control, which affects rotation speed. However, because the output voltage and frequency vary with speed, additional power electronics are needed for rectification of power stabilization, and this approach does not enable the expander to maintain optimal efficiency [113]. In addition, permanent magnet generators are expensive, which must be considered. In applications involving appropriate rotation speeds and low structural requirements, direct coupling may be used to simplify the system. For example, scroll expanders can be directly coupled with induction generators in a configuration that is particularly suitable for small-scale ORC systems [114].

In summary, the selection of the expander–generator coupling method should account not only for individual mechanical characteristics but also for system-level factors such as the speed control strategy, structural constraints, operational flexibility, and site-specific requirements.

Table 8. Comparison and applications of various control methods for expanders in ORC systems under off-design conditions.

Type	Positive Effects			Negative Effects			Application Fields
	Expander Rotation Speed	Evaporation Pressure	Stator Control	Expander Rotation Speed	Evaporation Pressure	Stator Control	
Turbine	No additional mechanism required	Easily adjustable evaporation ratio	Helps maintain the rotor inlet velocity to improve efficiency	Limited flow regulation range	Operation under off-design conditions	• Complex mechanical structure • Induced vibration	• Geothermal energy • Biomass energy
Volumetric	• Flexible speed control • Easy generator coupling		—	Excessive rotation speeds may increase wear, leakage, and noise and reduce efficiency		—	• Solar energy • Industrial waste heat recovery

Table 9. Summary of ORC installations in Taiwan from 2020 to 2025.

Year	Capacity (kW)	Type	Application	Installation Site
2020	980	Turbine	Mixed gas (low-pressure steam + CO_2)	Mailiao, Yunlin
2020	125	Screw	Industrial waste heat (steam)	Tashan Power Plant, Kinmen
2020	500	Turbine	Low-pressure steam	Dashe, Kaohsiung
2020	82	Screw	Industrial waste heat (steam)	Liuying Industrial Park, Tainan
2020	137	Screw	Industrial waste heat (steam)	Liuying Industrial Park, Tainan
2021	400	Turbine	Geothermal energy	Cingshui, Yilan
2021	550	Turbine	Geothermal energy	Jinlun, Taitung
2021	300	Turbine	Geothermal energy	Cingshui, Yilan
2022	680	Turbine	Industrial waste heat (steam)	Dashe, Kaohsiung
2022	190	Screw	Industrial waste heat (steam)	Dafa Industrial Park, Kaohsiung
2023	106	Screw	Industrial waste heat (liquid)	Mailiao, Yunlin
2023	250	Screw	Industrial waste heat (liquid)	Mailiao, Yunlin
2023	840	Turbine	Geothermal energy	Renze, Yilan
2023	270	Screw	Industrial waste heat (steam)	Pingnan Industrial Park, Pingtung
2023	196	Screw	Industrial waste heat (steam)	Liuying Industrial Park, Tainan
2023	250	Screw	Industrial waste heat (steam)	Hsinchu Science Park, Hsinchu
2023	68	Screw	Industrial waste heat (liquid)	Mailiao, Yunlin
2023	220	Screw	Industrial waste heat (liquid)	Mailiao, Yunlin
2023	486	Turbine	Industrial waste heat (steam)	Guanyin Industrial Park, Taoyuan
2023	10	Screw	Geothermal energy	Jinshan, New Taipei City
2024	585	Turbine	Geothermal energy	Jinlun, Taitung
2024	50	Screw	Industrial waste heat (liquid)	National Atomic Research Institute, Taoyuan
2024	893	Turbine	Industrial waste heat (steam)	Mailiao, Yunlin
2024	212	Screw	Heat transfer oil	Madou, Tainan
2025	200	Screw	Industrial waste heat (steam)	Tainan
2025	220	Screw	Industrial waste heat (liquid)	Mailiao, Yunlin
2025	250	Screw	Industrial waste heat (steam)	Hsinchu

5. Conclusions

ORC technology can convert low-grade heat into useful power. The expander, as a critical component in ORC systems, can be classified into turbo and volumetric types. This study provides an overview of the operating principles and application scenarios of commonly used expanders in ORC systems. Furthermore, this study highlights the influence of expander sealing on system performance, outlines potential enhancements, and discusses the applicable ranges of operational parameters. The key conclusions of this study are as follows:

(1) The performance of turbo expanders is substantially affected by blade geometry and operation conditions. The blade profile can be optimized using computational fluid dynamics software and meanline design

methods to increase isentropic efficiency. Additionally, the implementation of variable guide vanes, sliding-pressure control and partial admission techniques can improve operation stability and performance under off-design conditions.

(2) Scroll, vane, and screw expanders are the most extensively studied volumetric expanders. For scroll expanders, finite element analysis can be employed to investigate component deformation, with results indicating that thermal effects have a more substantial influence on component deformation than pressure loads do. Scroll expanders are typically suitable for applications with power outputs < 6 kW. Compared with TSEs, SSEs exhibit lower internal leakage and higher volumetric efficiency, operating within a rotation speed range of 1233–3200 rpm, rendering them well-suited to small-to-medium power capacity applications. By contrast, TSEs operate over a wider speed range of 1250–20,000 rpm and have greater adaptability, particularly for high-rotation-speed and medium- to large-scale applications. Among available volumetric expanders, vane expanders exhibit the lowest isentropic and volumetric efficiencies because of their structural design, which leads to considerable internal leakage. Consequently, extensive research has been conducted to address leakage reduction and enhance performance in these expanders.

(3) Turbo expanders exhibit higher isentropic efficiency and are suitable for operation under high-temperature and high mass flow rate conditions. By contrast, volumetric expanders are associated with lower costs and reduced operating rotation speeds, and they can accommodate working fluids in a two-phase state. Notably, volumetric expanders operate under high pressure ratios at low rotation speeds. Nevertheless, technical challenges such as those related to sealing performance, frictional losses, thermal expansion and thermal deformation, and material selection remain critical concerns that warrant further investigation to enable optimization of volumetric expanders.

(4) Volumetric expanders are commonly used in experimental studies because of their small scale, simple structure, and low cost. By contrast, turbo expanders, which have higher manufacturing costs and stricter structural requirements, are more frequently investigated through numerical simulations to evaluate the effects of design parameters on performance. In numerical modeling, turbo expanders are often integrated with thermodynamic cycle design to enable system-level optimization and efficiency assessments.

(5) This study presents a systematic review of expander technologies in ORC systems, with a focus on their operational principles, performance, and applicability. By summarizing the advantages, limitations, and performance enhancement strategies of the various expander types reported in the literature, this study provides a useful reference for expander selection, system design considerations, and future performance enhancements. The insights of this review can inform future research and facilitate the practical deployment of ORC systems in sustainable energy applications.

(6) ORC expanders must be capable of adapting to variable heat sources for maintaining system efficiency and stability. Although turbo expanders are typically efficient under their design conditions, they have limited tolerance of load fluctuations and require complex control strategies, such as variable guide vanes and partial admission, which increase their mechanical complexity and cost. Compared with turbo expanders, volumetric expanders, such as screw and scroll expanders, offer greater operational flexibility and are better suited for small- and medium-scale applications with fluctuating thermal loads. The control strategies used with volumetric expanders primarily involve regulation of the working fluid mass flow rate and evaporation pressure through pump frequency control to maintain appropriate superheat and match the expander's built-in volume ratio. Furthermore, the mechanical method of coupling used between the expander and generator (i.e., direct drive, belt transmission, or gearbox) not only affects rotation speed control but also influences the system's complexity, cost, and suitability for grid-connected or off-grid applications. These interdependent factors must be carefully considered during the design of ORC systems to ensure optimal performance across variable operating conditions.

Author Contributions: J.H.: writing—reviewing and editing, conceptualization, supervision; H.T.: data curation, writing—original draft preparation, visualization; Y.C.: writing—original draft preparation, data curation; C.C.: writing—original draft preparation, data curation; C.L.: writing—original draft preparation, data curation. All authors have read and agreed to the published version of the manuscript.

Funding: The authors gratefully acknowledge the financial support from the National Science and Technology Council (NSTC), Taiwan, under grant numbers NSTC111-2221-E-167-017-MY3 and NSTC113-2221-E-167-039-MY3. We also thank HanPower Energy Technology Co., Ltd. for providing valuable data on ORC installations in Taiwan, which contributed significantly to this study.

Institutional Review Board Statement: Not applicable.

Informed Consent Statement: Not applicable.

Data Availability Statement: Data will available on request.

Conflicts of Interest: The authors declare no conflict of interest.

References

1. Twidell, J. *Renewable Energy Resources*; Routledge: London, UK, 2021.
2. Tchanche, B.F.; Lambrinos, G.; Frangoudakis, A.; et al. Low-grade heat conversion into power using organic Rankine cycles—A review of various applications. *Renew. Sustain. Energy Rev.* **2011**, *15*, 3963–3979.
3. Wieland, C.; Dawo, F.; Schifflechner, C.; et al. Market report on Organic Rankine Cycle power systems: Recent developments and outlook. In Proceedings of the 6th International Seminar on ORC Power Systems, Virtual, 11–13 October 2021.
4. Tartière, T.; Astolfi, M. A world overview of the organic Rankine cycle market. *Energy Procedia* **2017**, *129*, 2–9.
5. Quoilin, S.; Van Den Broek, M.; Declaye, S.; et al. Techno-economic survey of Organic Rankine Cycle (ORC) systems. *Renew. Sustain. Energy Rev.* **2013**, *22*, 168–186.
6. Liu, B.T.; Chien, K.H.; Wang, C.C. Effect of working fluids on organic Rankine cycle for waste heat recovery. *Energy* **2004**, *29*, 1207–1217.
7. White, M.; Sayma, A.I. Improving the economy-of-scale of small organic rankine cycle systems through appropriate working fluid selection. *Appl. Energy* **2016**, *183*, 1227–1239.
8. Bianchi, M.; Branchini, L.; De Pascale, A.; et al. Performance and total warming impact assessment of pure fluids and mixtures replacing HFCs in micro-ORC energy systems. *Appl. Therm. Eng.* **2022**, *203*, 117888.
9. Qiu, K.; Thomas, M.; Douglas, M. Investigation of a scroll expander driven by compressed air and its potential applications to ORC. *Appl. Therm. Eng.* **2018**, *135*, 109–115.
10. Feng, X.; Shi, F.; Qiao, G.; et al. *Integrating Organic Rankine Cycle with Thermoelectric Generator in Various Applications Utilizing Low-Grade Energy: A Review*; Sustainable Energy Technologies and Assessments; Elsevier: Amsterdam, The Netherlands, 2024.
11. Wu, T.; Wei, X.; Meng, X.; et al. Experimental study of operating load variation for organic Rankine cycle system based on radial inflow turbine. *Appl. Therm. Eng.* **2020**, *166*, 114641.
12. Imran, M.; Usman, M.; Park, B.S.; et al. Volumetric expanders for low grade heat and waste heat recovery applications. *Renew. Sustain. Energy Rev.* **2016**, *57*, 1090–1109.
13. Zheng, Y.; Hu, D.; Cao, Y.; et al. Preliminary design and off-design performance analysis of an Organic Rankine Cycle radial-inflow turbine based on mathematic method and CFD method. *Appl. Therm. Eng.* **2017**, *112*, 25–37.
14. Dixon, S.L.; Eng, B.; Hall, C.A. *Fluid Mechanics and Thermodynamics of Turbomachinery*, 7th ed.; Elsevier: Amsterdam, The Netherlands, 2014.
15. Bao, J.; Zhao, L. A review of working fluid and expander selections for organic Rankine cycle. *Renew. Sustain. Energy Rev.* **2013**, *24*, 325–342.
16. Sauret, E.; Gu, Y. Three-dimensional off-design numerical analysis of an organic Rankine cycle radial-inflow turbine. *Appl. Energy* **2014**, *135*, 202–211.
17. Wang, Z.; Xie, B.; Xia, X.; et al. Entropy production analysis of a radial inflow turbine with variable inlet guide vane for ORC application. *Energy* **2023**, *265*, 126313.
18. Al Jubori, A.; Daabo, A.; Al-Dadah, R.K.; et al. Development of micro-scale axial and radial turbines for low-temperature heat source driven organic Rankine cycle. *Energy Convers. Manag.* **2016**, *130*, 141–155.
19. Yao, Y.; Fang, S.; Zhu, S.; et al. Optimal design and tip leakage flow characteristics analysis of radial inflow turbine used in organic Rankine and vapor compression refrigeration system. *Energy* **2024**, *301*, 131668.
20. Dong, B.; Xu, G.; Luo, X.; et al. Analysis of the supercritical organic Rankine cycle and the radial turbine design for high temperature applications. *Appl. Therm. Eng.* **2017**, *123*, 1523–1530.
21. Kim, D.Y.; Kim, Y.T. Preliminary design and performance analysis of a radial inflow turbine for organic Rankine cycles. *Appl. Therm. Eng.* **2017**, *120*, 549–559.
22. Du, Y.; Yang, Y.; Hu, D.; et al. Off-design performance comparative analysis between basic and parallel dual-pressure organic Rankine cycles using radial inflow turbines. *Appl. Therm. Eng.* **2018**, *138*, 18–34.
23. Xia, J.; Wang, J.; Wang, H.; et al. Three-dimensional performance analysis of a radial-inflow turbine for an organic Rankine cycle driven by low grade heat source. *Energy Convers. Manag.* **2018**, *169*, 22–33.
24. Quan, Y.; Liu, J.; Zhang, C.; et al. Aerodynamic design of an axial impulse turbine for the high-temperature organic Rankine cycle. *Appl. Therm. Eng.* **2020**, *167*, 114708.
25. Sarmiento, A.L.E.; Camacho, R.G.R.; de Oliveira, W.; et al. Design and off-design performance improvement of a radial-inflow turbine for ORC applications using metamodels and genetic algorithm optimization. *Appl. Therm. Eng.* **2021**, *183*, 116197.

26. Li, B.; Xie, H.; Sun, L.; et al. Optimization design of radial inflow turbine combined with mean-line model and CFD analysis for geothermal power generation. *Energy* **2024**, *291*, 130452.
27. Yu, H.; Helland, H.; Yu, X.; et al. Optimal design and operation of an Organic Rankine Cycle (ORC) system driven by solar energy with sensible thermal energy storage. *Energy Convers. Manag.* **2021**, *244*, 114494.
28. Kupka, D.; Koloničný, J.; Pejchal, J. Development of an axial impulse turbine for a small-scale ORC system. *Results Eng.* **2025**, *25*, 103994.
29. Al Jubori, A.M.; Al-Dadah, R.; Mahmoud, S. An innovative small-scale two-stage axial turbine for low-temperature organic Rankine cycle. *Energy Convers. Manag.* **2017**, *144*, 18–33.
30. Witanowski, Ł.; Klonowicz, P.; Lampart, P.; et al. Multi-objective optimization of the ORC axial turbine for a waste heat recovery system working in two modes: Cogeneration and condensation. *Energy* **2023**, *264*, 126187.
31. Yang, Y.; Huo, Y.; Xia, W.; et al. Construction and preliminary test of a geothermal ORC system using geothermal resource from abandoned oil wells in the Huabei oilfield of China. *Energy* **2017**, *140*, 633–645.
32. Sun, H.; Qin, J.; Yan, P.; et al. Performance evaluation of a partially admitted axial turbine using R245fa, R123 and their mixtures as working fluid for small-scale organic Rankine cycle. *Energy Convers. Manag.* **2018**, *171*, 925–935.
33. Al Jubori, A.M.; Al-Dadah, R.K.; Mahmoud, S.; et al. Modelling and parametric analysis of small-scale axial and radial-outflow turbines for Organic Rankine Cycle applications. *Appl. Energy* **2017**, *190*, 981–996.
34. Peng, N.; Wang, E.; Meng, F. Off-design performance comparison of single-stage axial turbines using CO_2 and zeotropic mixture for low-temperature heat source. *Energy Convers. Manag.* **2020**, *213*, 112838.
35. Sun, H.; Qin, J.; Hung, T.C.; et al. Performance analysis of low speed axial impulse turbine using two type nozzles for small-scale organic Rankine cycle. *Energy* **2019**, *169*, 1139–1152.
36. Naas, T.T.; Telha, M.; Laib, L.; et al. Performance enhancement of three-stage axial turbine for Clean Organic Rankine Cycle system driven by low-temperature heat source. *Clean. Eng. Technol.* **2021**, *5*, 100336.
37. Klun, M.; Guzović, Z.; Rašković, P. Innovative small axial multistage turbine with partial admission for bottoming ORC. *Energy Rep.* **2021**, *7*, 9069–9093.
38. Alshammari, F.; Pesyridis, A.; Elashmawy, M. Turbine optimization potential to improve automotive Rankine cycle performance. *Appl. Therm. Eng.* **2021**, *186*, 116559.
39. Zengin, İ.; Erdoğan, B.; Benim, A.C. CFD and Taguchi based optimization of air driven single stage partial admission axial turbine blade profiles. *Energy* **2024**, *290*, 130333.
40. Guan, Y.; Li, W.; Zhu, Y.; et al. Aerodynamic performance and flow characteristics of a compressed air energy storage axial turbine with nozzle governing. *J. Energy Storage* **2023**, *63*, 106967.
41. Lemort, V.; Quoilin, S.; Cuevas, C.; et al. Testing and modeling a scroll expander integrated into an Organic Rankine Cycle. *Appl. Therm. Eng.* **2009**, *29*, 3094–3102.
42. Zhu, Y.; Jiang, L.; Jin, V.; et al. Impact of built-in and actual expansion ratio difference of expander on ORC system performance. *Appl. Therm. Eng.* **2014**, *71*, 548–558.
43. Kim, Y.M.; Shin, D.G.; Kim, C.G. Optimization of design pressure ratio of positive displacement expander for vehicle engine waste heat recovery. *Energies* **2014**, *7*, 6105–6117.
44. Tassou, S.A.; Qureshi, T.Q. Comparative performance evaluation of positive displacement compressors in variable-speed refrigeration applications. *Int. J. Refrig.* **1998**, *21*, 29–41.
45. Wang, Z.; Wang, Z.; Wang, J.; et al. Theoretical and experimental study on thermodynamic performance of single screw refrigeration compressor with Multicolumn Envelope Meshing Pair. *Appl. Therm. Eng.* **2016**, *103*, 139–149.
46. Lecompte, S.; Huisseune, H.; Van Den Broek, M.; et al. Review of organic Rankine cycle (ORC) architectures for waste heat recovery. *Renew. Sustain. Energy Rev.* **2015**, *47*, 448–461.
47. Qiu, G.; Liu, H.; Riffat, S. Expanders for micro-CHP systems with organic Rankine cycle. *Appl. Therm. Eng.* **2011**, *31*, 3301–3307.
48. Capata, R.; Pantano, F. Expander design procedures and selection criterion for small rated organic rankine cycle systems. *Energy Sci. Eng.* **2020**, *8*, 3380–3414.
49. Declaye, S.; Quoilin, S.; Guillaume, L.; et al. Experimental study on an open-drive scroll expander integrated into an ORC (Organic Rankine Cycle) system with R245fa as working fluid. *Energy* **2013**, *55*, 173–183.
50. Ma, X.; Lv, X.; Li, C.; et al. Accurate modelling of the scroll expander via a mechanism-incorporated data-driven method. *Int. J. Refrig.* **2023**, *155*, 32–46.
51. Yanagisawa, T.; Shimizu, T.; Fukuta, M.; et al. Study on fundamental performance of scroll expander. *Trans. Jpn. Soc. Mech. Eng. Ser. B* **1988**, *54*, 2798–2803.
52. Hsieh, J.C.; Chen, Y.H.; Hsieh, Y.C. Experimental study of an organic Rankine cycle with a variable-rotational-speed scroll expander at various heat source temperatures. *Energy* **2023**, *270*, 126956.
53. Hsieh, J.C.; Hsieh, Y.C.; Chen, Y.H. Effect of superheat degree on the performance of an organic Rankine cycle system that utilizes a wet working fluid. *Energy Sci. Eng.* **2024**, *12*, 5019–5030.

54. Wu, Z.; Pan, D.; Gao, N.; et al. Experimental testing and numerical simulation of scroll expander in a small scale organic Rankine cycle system. *Appl. Therm. Eng.* **2015**, *87*, 529–537.
55. Fukuta, M.; Yanagisawa, T.; Kosuda, O.; Ogi, Y. Performance of Scroll Expander for CO_2 Refrigeration Cycle. In Proceedings of the International Compressor Engineering Conference, Purdue University, West Lafayette, IN, USA, 17–20 July 2006; Purdue University Press: West Lafayette, IN, USA, 2006.
56. Gao, P.; Jiang, L.; Wang, L.W.; et al. Simulation and experiments on an ORC system with different scroll expanders based on energy and exergy analysis. *Appl. Therm. Eng.* **2015**, *75*, 880–888.
57. Kosmadakis, G.; Mousmoulis, G.; Manolakos, D.; et al. Development of open-drive scroll expander for an Organic Rankine Cycle (ORC) engine and first test results. *Energy Procedia* **2017**, *129*, 371–378.
58. Cambi, M.; Tascioni, R.; Cioccolanti, L.; et al. Converting a commercial scroll compressor into an expander: Experimental and analytical performance evaluation. *Energy Procedia* **2017**, *129*, 363–370.
59. Giuffrida, A. A theoretical study on the performance of a scroll expander in an organic Rankine cycle with hydrofluoroolefins (HFOs) in place of R245fa. *Energy* **2018**, *161*, 1172–1180.
60. Yang, J.; Sun, Z.; Yu, B.; et al. Modeling and optimization criteria of scroll expander integrated into organic Rankine cycle for comparison of R1233zd (E) as an alternative to R245fa. *Appl. Therm. Eng.* **2018**, *141*, 386–393.
61. Dumont, O.; Parthoens, A.; Dickes, R.; et al. Experimental investigation and optimal performance assessment of four volumetric expanders (scroll, screw, piston and roots) tested in a small-scale organic Rankine cycle system. *Energy* **2018**, *165*, 1119–1127.
62. Ziviani, D.; James, N.A.; Accorsi, F.A.; et al. Experimental and numerical analyses of a 5 kWe oil-free open-drive scroll expander for small-scale organic Rankine cycle (ORC) applications. *Appl. Energy* **2018**, *230*, 1140–1156.
63. Fatigati, F.; Cipollone, R. Experimental and theoretical assessment of the effects of electrical load variation on the operability of a small-scale Organic Rankine Cycle (ORC)-based unit equipped with a hermetic scroll expander. *Energy* **2024**, *311*, 133318.
64. Hijriawan, M.; Pambudi, N.A.; Wijayanto, D.S.; et al. Experimental analysis of R134a working fluid on Organic Rankine Cycle (ORC) systems with scroll-expander. *Eng. Sci. Technol. Int. J.* **2022**, *29*, 101036.
65. Wang, Z.; Pan, H.; Xia, X.; et al. Experimental investigation on steady and dynamic performance of organic Rankine cycle with R245fa/R141b under different cooling and expander speed conditions. *Energy* **2022**, *241*, 122511.
66. Zhang, H.H.; Zhang, Y.F.; Feng, Y.Q.; et al. The parametric analysis on the system behaviors with scroll expanders employed in the ORC system: An experimental comparison. *Energy* **2023**, *268*, 126713.
67. Feng, Y.Q.; Liang, H.J.; Xu, K.; et al. Experimental study on the performance of a great progress 10 kW organic Rankine cycle for low-grade heat source based on scroll-type expander. *Energy* **2023**, *284*, 128627.
68. Zhen, K.; Shi, L.; Zhang, Y.; et al. Performance prediction and regression analysis of scroll expander based on response surface methodology. *Case Stud. Therm. Eng.* **2024**, *60*, 104766.
69. Wronski, J.; Imran, M.; Skovrup, M.J.; et al. Experimental and numerical analysis of a reciprocating piston expander with variable valve timing for small-scale organic Rankine cycle power systems. *Appl. Energy* **2019**, *247*, 403–416.
70. Oudkerk, J.F.; Lemort, V. Detailed experimental and model-based analysis of a swash-plate piston expander for ORC application. *Front. Energy Res.* **2020**, *8*, 107.
71. Zheng, N.; Zhao, L.; Wang, X.D.; et al. Experimental verification of a rolling-piston expander that applied for low-temperature Organic Rankine Cycle. *Appl. Energy* **2013**, *112*, 1265–1274.
72. Han, Y.; Kang, J.; Zhang, G.; et al. Performance evaluation of free piston compressor coupling organic Rankine cycle under different operatinSg conditions. *Energy Convers. Manag.* **2014**, *86*, 340–348.
73. Chatzopoulou, M.A.; Simpson, M.; Sapin, P.; et al. Off-design optimisation of organic Rankine cycle (ORC) engines with piston expanders for medium-scale combined heat and power applications. *Appl. Energy* **2019**, *238*, 1211–1236.
74. Bianchi, M.; Branchini, L.; Casari, N.; et al. Experimental analysis of a micro-ORC driven by piston expander for low-grade heat recovery. *Appl. Therm. Eng.* **2019**, *148*, 1278–1291.
75. Bianchi, M.; Branchini, L.; De Pascale, A.; et al. Application and comparison of semi-empirical models for performance prediction of a kW-size reciprocating piston expander. *Appl. Energy* **2019**, *249*, 143–156.
76. Bianchi, M.; Branchini, L.; De Pascale, A.; et al. Replacement of R134a with low-GWP fluids in a kW-size reciprocating piston expander: Performance prediction and design optimization. *Energy* **2020**, *206*, 118174.
77. Han, Y.; Zhang, Y.; Zuo, T.; et al. Experimental study and energy loss analysis of an R245fa organic Rankine cycle prototype system with a radial piston expander. *Appl. Therm. Eng.* **2020**, *169*, 114939.
78. Gao, J.; Ma, C.; Tian, G.; et al. Numerical investigations of an opposed rotary piston expander for the purpose of the applications to a small-scale Rankine cycle. *Appl. Therm. Eng.* **2021**, *182*, 116157.
79. Wei, J.; Hua, Q.; Wang, J.; et al. Overview of the Development and Application of the Twin Screw Expander. *Energies* **2020**, *13*, 6586.
80. Ziviani, D.; Bell, I.; van den Broek, M.; De Paepe, M. Comprehensive Model of a Single-Screw Expander for ORC-

Systems. In Proceedings of the International Compressor Engineering Conference, Purdue University, West Lafayette, IN, USA, 14–17 July 2014; Purdue University Press: West Lafayette, IN, USA, 2014.
81. Tian, Y.; Wang, Z.; Liu, Z.; et al. Two-phase Flow Characteristics and Leakage in the Shaft Seal of Steam Screw Expanders. *Int. J. Refrig.* **2025**, *172*, 214–227.
82. Tang, H.; Wu, H.; Wang, X.; et al. Performance study of a twin-screw expander used in a geothermal organic Rankine cycle power generator. *Energy* **2015**, *90*, 631–642.
83. Lei, B.; Wang, W.; Wu, Y.T.; et al. Development and experimental study on a single screw expander integrated into an Organic Rankine Cycle. *Energy* **2016**, *116*, 43–52.
84. Giuffrida, A. Improving the semi-empirical modelling of a single-screw expander for small organic Rankine cycles. *Appl. Energy* **2017**, *193*, 356–368.
85. Xia, G.D.; Zhang, Y.Q.; Wu, Y.T.; et al. Experimental study on the performance of single-screw expander with different inlet vapor dryness. *Appl. Therm. Eng.* **2015**, *87*, 34–40.
86. Ziviani, D.; Groll, E.A.; Braun, J.E.; et al. Review and update on the geometry modeling of single-screw machines with emphasis on expanders. *Int. J. Refrig.* **2018**, *92*, 10–26.
87. Bianchi, G.; Kennedy, S.; Zaher, O.; et al. Numerical modeling of a two-phase twin-screw expander for Trilateral Flash Cycle applications. *Int. J. Refrig.* **2018**, *88*, 248–259.
88. Song, X.; Wu, Y.; Shen, L.; et al. Comparative experimental analysis of the effect of lubricant viscosity on the performance of a single-screw expander with different structures. *J. Energy Storage* **2022**, *52*, 104958.
89. Yang, K.; Zhang, H.; Song, S.; et al. Performance analysis of the vehicle diesel engine-ORC combined system based on a screw expander. *Energies* **2014**, *7*, 3400–3419.
90. Zhang, Y.Q.; Wu, Y.T.; Xia, G.D.; et al. Development and experimental study on organic Rankine cycle system with single-screw expander for waste heat recovery from exhaust of diesel engine. *Energy* **2014**, *77*, 499–508.
91. Hsu, S.W.; Chiang HW, D.; Yen, C.W. Experimental investigation of the performance of a hermetic screw-expander organic Rankine cycle. *Energies* **2014**, *7*, 6172–6185.
92. Ziviani, D.; Gusev, S.; Lecompte, S.; et al. Characterizing the performance of a single-screw expander in a small-scale organic Rankine cycle for waste heat recovery. *Appl. Energy* **2016**, *181*, 155–170.
93. Ziviani, D.; Gusev, S.; Lecompte, S.; et al. Optimizing the performance of small-scale organic Rankine cycle that utilizes a single-screw expander. *Appl. Energy* **2017**, *189*, 416–432.
94. Nikolov, A.; Brümmer, A. Investigating a small oil-flooded twin-screw expander for waste-heat utilisation in organic rankine cycle systems. *Energies* **2017**, *10*, 869.
95. Eyerer, S.; Dawo, F.; Rieger, F.; et al. Experimental and numerical investigation of direct liquid injection into an ORC twin-screw expander. *Energy* **2019**, *178*, 867–878.
96. Guo, Z.; Zhang, C.; Wu, Y.; et al. Numerical optimization of intake and exhaust structure and experimental verification on single-screw expander for small-scale ORC applications. *Energy* **2020**, *199*, 117478.
97. Zhao, Z.; Zhang, J.; Wang, G.; et al. Research and clearance analysis on of steam twin-screw expander employed in indutrial waste heat recovery. *Energy* **2024**, *312*, 133439.
98. Wang, H.X.; Lei, B.; Wu, Y.T.; et al. Experimental investigation and machine learning applications of a quasi-two-stage single screw expander integrated into an Organic Rankine Cycle. *Appl. Therm. Eng.* **2025**, *268*, 125896.
99. Vodicka, V.; Novotny, V.; Zeleny, Z.; et al. Theoretical and experimental investigations on the radial and axial leakages within a rotary vane expander. *Energy* **2019**, *189*, 116097.
100. Naseri, A.; Norris, S.; Subiantoro, A. Experimental investigation of a prototype semi-dry revolving vane expander: Design challenges and performance criteria. *Energy* **2020**, *205*, 118063.
101. Vodicka, V.; Novotny, V.; Mascuch, J.; et al. Impact of major leakages on characteristics of a rotary vane expander for ORC. *Energy Procedia* **2017**, *129*, 387–394.
102. Yang, B.; Sun, S.; Peng, X.; Guo, B.; Xing, Z. Modeling and Experimental Investigation on the Internal Leakage in a CO_2 Rotary Vane Expander. In Proceedings of the International Compressor Engineering Conference, Purdue University, West Lafayette, IN, USA, 14–17 July 2008; Purdue University Press: West Lafayette, IN, USA, 2008.
103. Naseri, A.; Norris, S.E.; Subiantoro, A. Experimental investigation of leakage in the modified revolving vane expander. *J. Fluids Eng.* **2021**, *143*, 071206.
104. Mahmoud, A.M.; Sherif, S.A.; Lear, W.E. Frictional and internal leakage losses in rotary-vane two-phase refrigerating expanders. *J. Energy Resour. Technol.* **2010**, *132*, 021007.
105. Jia, X.; Zhang, B.; Pu, L.; et al. Improved rotary vane expander for trans-critical CO_2 cycle by introducing high-pressure gas into the vane slots. *Int. J. Refrig.* **2011**, *34*, 732–741.
106. Yang, B.; Peng, X.; He, Z.; et al. Experimental investigation on the internal working process of a CO2 rotary vane expander. *Appl. Therm. Eng.* **2009**, *29*, 2289–2296.
107. Casari, N.; Fadiga, E.; Pinelli, M.; et al. Investigation of flow characteristics in a single screw expander: A numerical

approach. *Energy* **2020**, *213*, 118730.

108. Mascuch, J.; Novotny, V.; Vodicka, V.; et al. Experimental development of a kilowatt-scale biomass fired micro–CHP unit based on ORC with rotary vane expander. *Renew. Energy* **2020**, *147*, 2882–2895.
109. Naseri, A.; Moradi, R.; Norris, S.; et al. Experimental investigation of a revolving vane expander in a micro-scale organic Rankine cycle system for low-grade waste heat recovery. *Energy* **2022**, *253*, 124174.
110. Fatigati, F.; Vittorini, D.; Di Bartolomeo, M.; et al. Experimental and theoretical analysis of a micro-cogenerative solar ORC-based unit equipped with a variable speed sliding rotary vane expander. *Energy Convers. Manag. X* **2023**, *20*, 100428.
111. Vittorini, D.; Antonini, A.; Cipollone, R.; et al. Solar thermal-based orc power plant for micro cogeneration–performance analysis and control strategy. *Energy Procedia* **2018**, *148*, 774–781.
112. Fu, B.R.; Lee, Y.R.; Hsieh, J.C. Design, construction, and preliminary results of a 250-kW organic Rankine cycle system. *Appl. Therm. Eng.* **2015**, *80*, 339–346.
113. Chang, J.C.; Hung, T.C.; He, Y.L.; et al. Experimental study on low-temperature organic Rankine cycle utilizing scroll type expander. *Appl. Energy* **2015**, *155*, 150–159.
114. Jiang, Y.; Feng, Y.; Tian, S.; et al. Experimental and numerical optimization of a scroll expander for small-scale ORC systems using pure and mixture working fluids. *Energy* **2025**, *333*, 137333.